Supporting Information

A dual-function flexible pressure/humidity sensitive sensor based on polyaniline-coated melamine sponge

Jinqiang Sun[a§], Hongxing Li[a§], Xiaolin Ma[a] Yuanyuan Li[a], Lizhong Liu[a], Lulu Song[a] Xueke Wang[a], Xiaoxiao Deng[a], Chun Yu[a,*], Yi Zhao[a,*]

[a] Strait Institute of Flexible Electronics (SIFE, Future Technologies), Fujian Key Laboratory of Flexible Electronics, Fujian Normal University and Strait Laboratory of Flexible Electronics (SLoFE), Fuzhou 350117, China.

§ These authors contributed to the work equally.

* Corresponding author

Email: ifecyu@fjnu.edu.cn; ifeyzhao@fjnu.edu.cn.

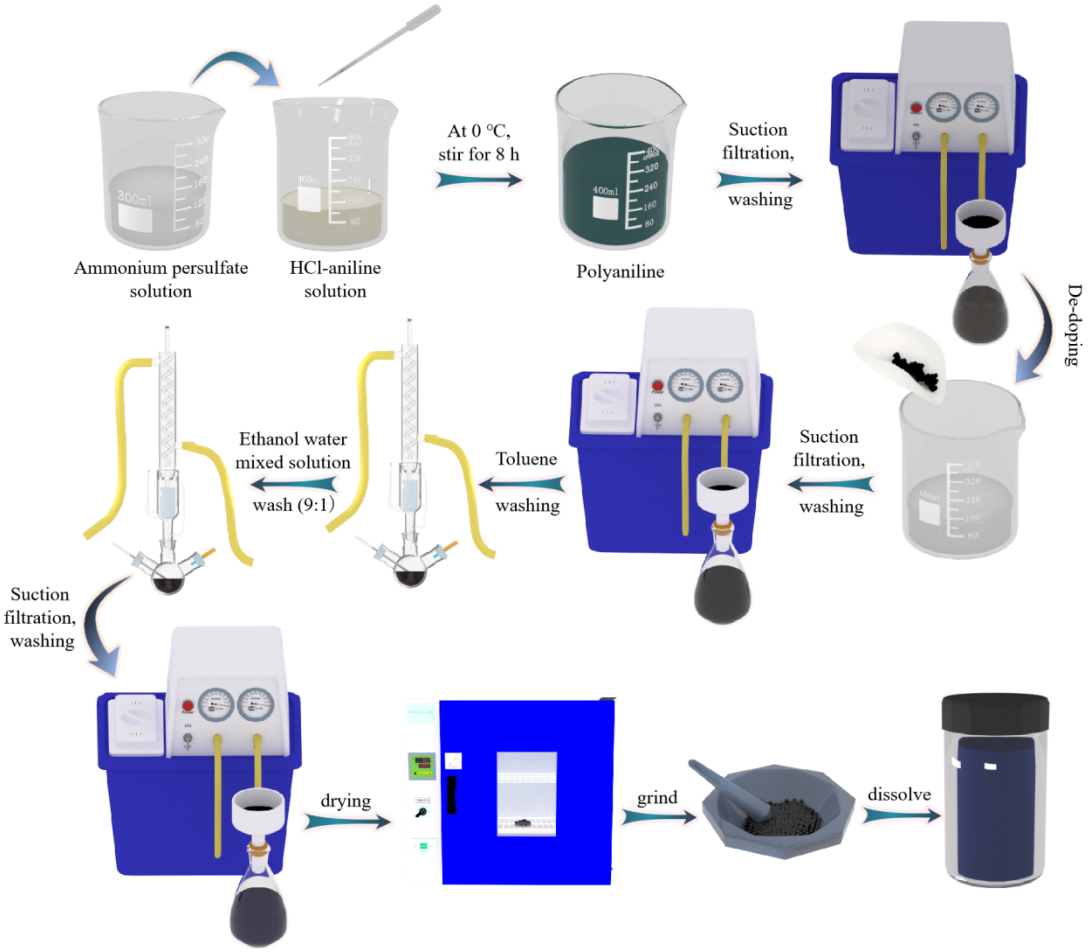

Fig. S1 Flow chart of preparation of PANI solution.

As shown in Fig. S1, the PANI powder was first synthesized using chemical oxidative polymerization, dissolved, and then centrifuged to obtain a uniform PANI solution. Specifically:

Synthesis of the PANI Solution: Firstly, 11.4 ml of purified aniline monomer, obtained through vacuum distillation, was added to an aqueous hydrochloric acid solution (125 ml of deionized water, 12.5 ml of concentrated hydrochloric acid) to form an aniline solution. Next, 14.25 g of ammonium persulfate was dissolved in 125 ml of aqueous solution, and the two solutions were separately ice-bathed for ten minutes to ensure the reaction proceeded at a low temperature. After that, the ammonium persulfate solution was slowly dripped into the aniline solution (the polymerization of aniline is exothermic, and if the dripping speed is too fast, the reaction solution temperature will rise, which cannot be controlled at around 0°C, leading to uneven polymerization degree of the synthesized PANI). Subsequently, the oxidative polymerization of aniline monomer was initiated under ice-bath conditions (~0°C) with

continuous stirring. After 8 hours of polymerization, the aniline monomer was converted into green PANI. Then, the reaction system was subjected to vacuum filtration, and the PANI was washed multiple times with ethanol and deionized water to remove excess impurities.

Dedoping and Purification: Since hydrochloric acid was initially added to the aniline solution, the resulting product was hydrochloric acid-doped PANI. The doped ions (H^+) in the PANI were removed by soaking in concentrated ammonia water for 12 hours.

Vacuum filtration and washing: The de-doped PANI was filtered and washed to neutrality with deionized water to obtain emeraldine base PANI powder. Afterwards, the emeraldine base PANI powder was washed separately with toluene solution and ethanol aqueous solution (ethanol: water = 9:1) under N_2 protection for 72 hours to remove impurities and oligomers from the PANI, resulting in higher purity and more uniform chain length PANI powder. Subsequently, the PANI powder was washed again with a large amount of deionized water and ethanol using vacuum filtration. Finally, the obtained PANI material needs to be dried to remove residual moisture and organic solvents, ensuring the stability and reliability of the material. Then, the dried PANI powder was ground in a mortar, and 1 g of PANI powder was dissolved in 40 ml of N-methylpyrrolidone solvent and stirred for one day to make the PANI dissolve completely, obtaining a PANI solution. Finally, the PANI solution was separated and purified using a centrifuge to obtain a homogeneous PANI supernatant.

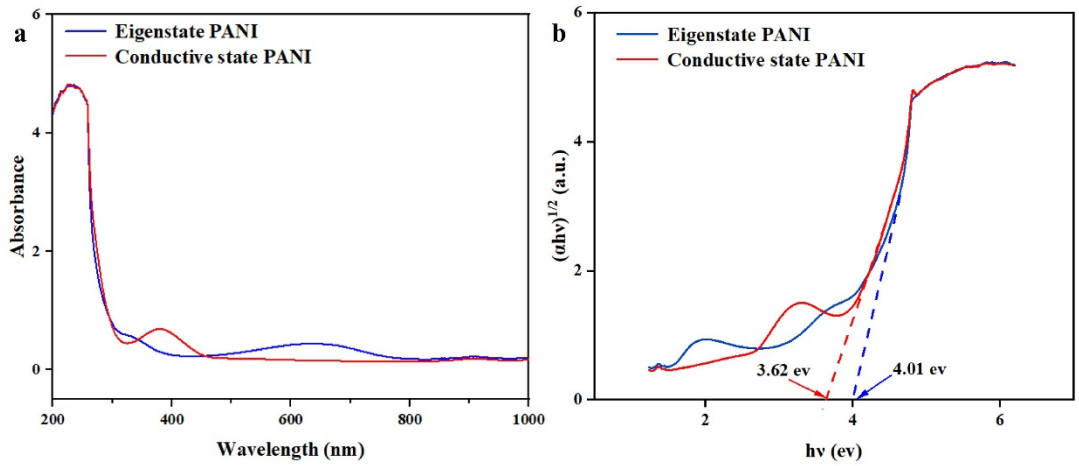

Fig. S2 a) Comparison of the UV spectra of intrinsic and conductive PANI, b) Bandgap calculation of intrinsic and conductive PANI using the Tauc plot method.

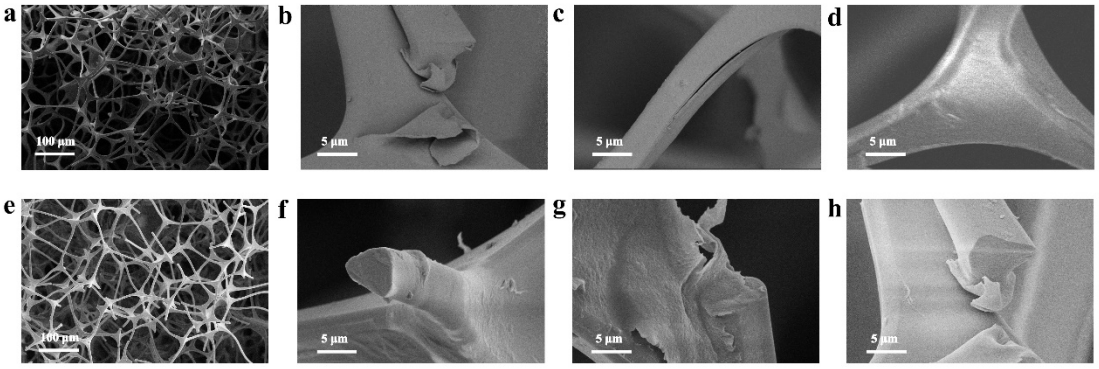

Fig. S3 SEM images of polyaniline sponge: a-d) before humidity and pressure cycling tests, e-f) after humidity and pressure cycling tests.

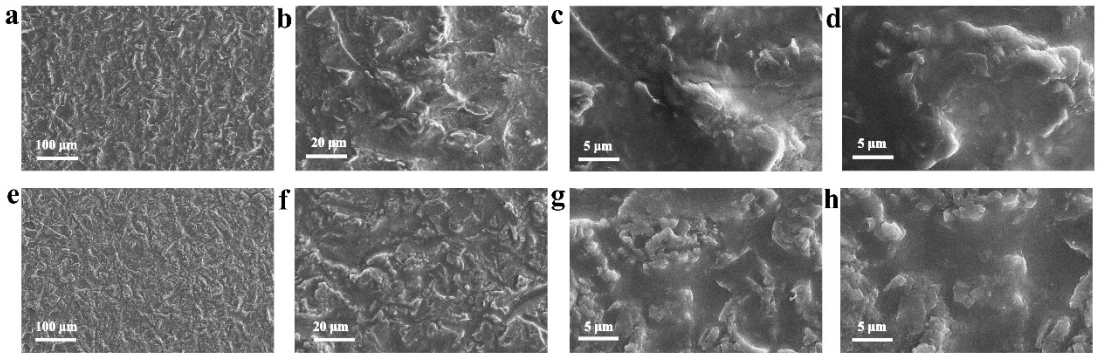

Fig. S4 SEM images of polyaniline film: a-d) before humidity tests, e-f) after humidity tests.

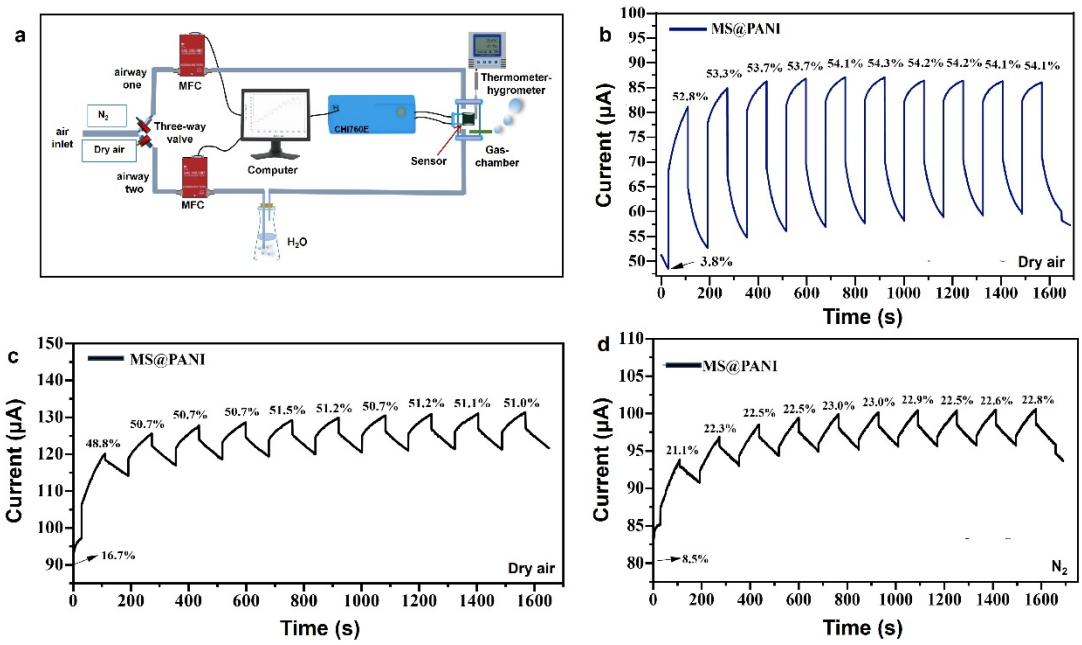

Fig. S5 a) Schematic diagram of the humidity sensing performance testing device for PANI films. b) Current variation curve of the PANI film during ten cycles of testing under dry air background. c) Current response curve of the MS@PANI sensor during ten cycles under dry air background. d) Current response curve of the MS@PANI sensor during ten cycles under N_2 background.

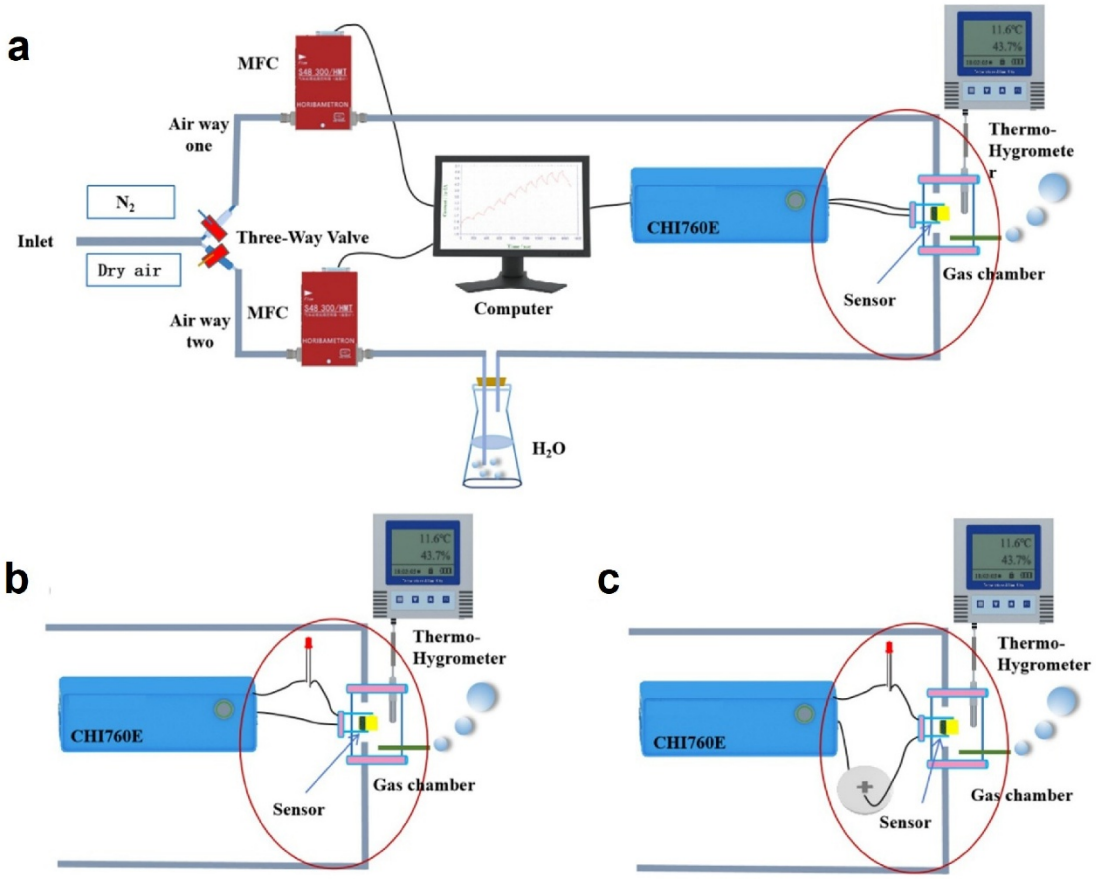

Fig. S6 (a-c) Circuit connection diagrams for humidity sensing performance testing of the MS@PANI sensor under different conditions.

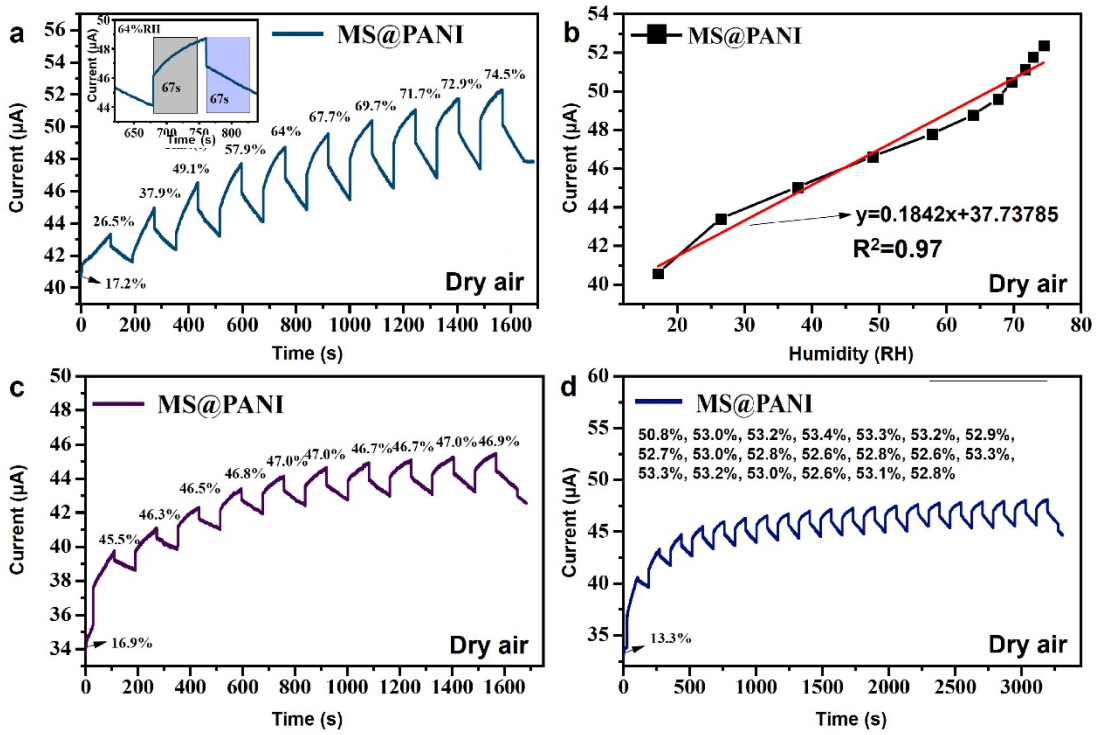

Fig. S7 Under dry air background, the MS@PANI sensor is connected to an LED light. a) Stepwise humidity current response curve. b) Fitting curve of current versus relative humidity. c) Ten cycles of testing. d) Twenty cycles of testing.

Fig. S4a illustrates the stepwise humidity current response curve for the MS@PANI sensor when connected to an LED light. The inset reveals that, with this circuit setup, both the response time and recovery time of the MS@PANI sensor at 64.0% RH are 67 s. A linear fit was conducted for the current values and relative humidity from 17.2% RH to 74.5% RH in this application circuit, indicating a strong linear correlation, as depicted in Fig. S3b. Fig. S4c presents the outcomes of ten cyclic tests carried out on the MS@PANI sensor in series with an LED light at approximately 47% RH. Likewise, Fig. S4d shows the results of twenty cyclic tests performed at around 52% RH. These findings underscore the sensor's excellent linear recognition capability (0.18 μA/%RH) and its good reproducibility in response to humidity.

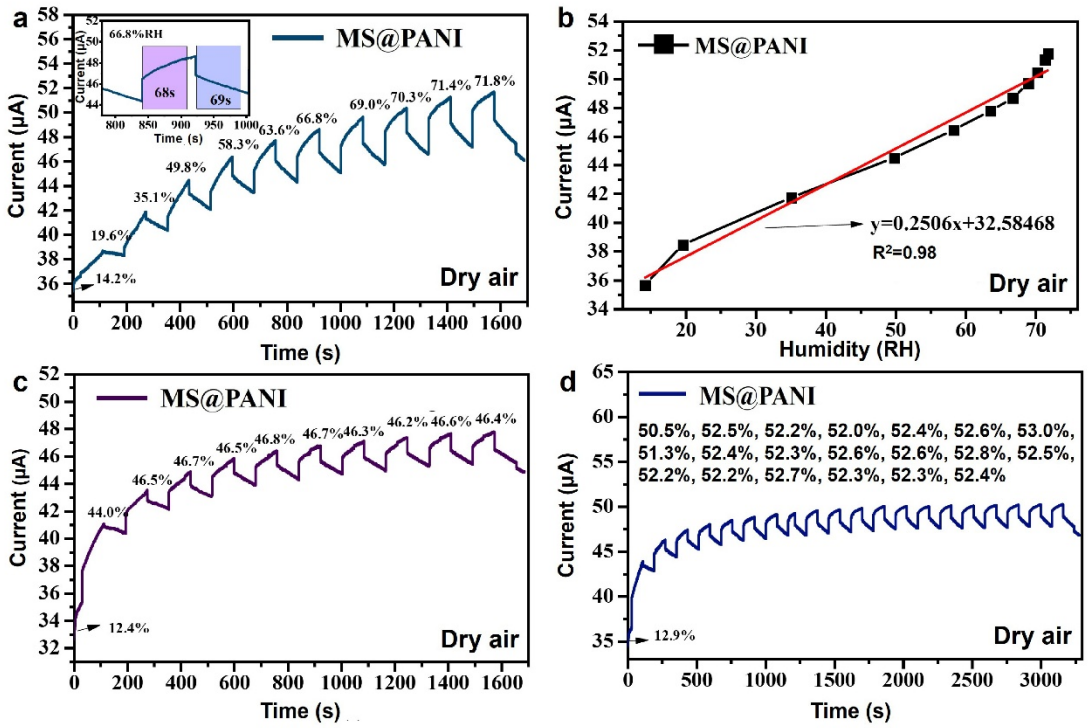

Fig. S8 Under dry air background, the MS@PANI sensor is connected in series to an LED light and powered by a commercial battery within the testing circuit. a) Stepwise humidity current response curve. b) Fitting curve of current versus relative humidity. c) Ten cycles of testing. d) Twenty cycles of testing.

Fig. S5a presents the stepwise humidity current response curve of the MS@PANI sensor connected in series to an LED light and powered by a commercial battery. The inset highlights that, under this circuit configuration, the response time and recovery time of the MS@PANI sensor at 66.8 %RH humidity are 68 s and 69 s, respectively. Fig. S5b shows the linear fitting of the sensor's current values relative to humidity across an environment ranging from 14.2 %RH to 71.8 %RH. Its linear correlation coefficient R^2 is 0.98, and its sensitivity is 0.25 μA/%RH. Fig. S5c demonstrates the results of ten cyclic tests performed on the MS@PANI sensor at approximately 46%RH, while Fig. S5d shows the outcomes of twenty cyclic tests conducted under approximately 52%RH conditions. The results from both repeatability tests confirm that the sensor exhibits excellent reproducibility.

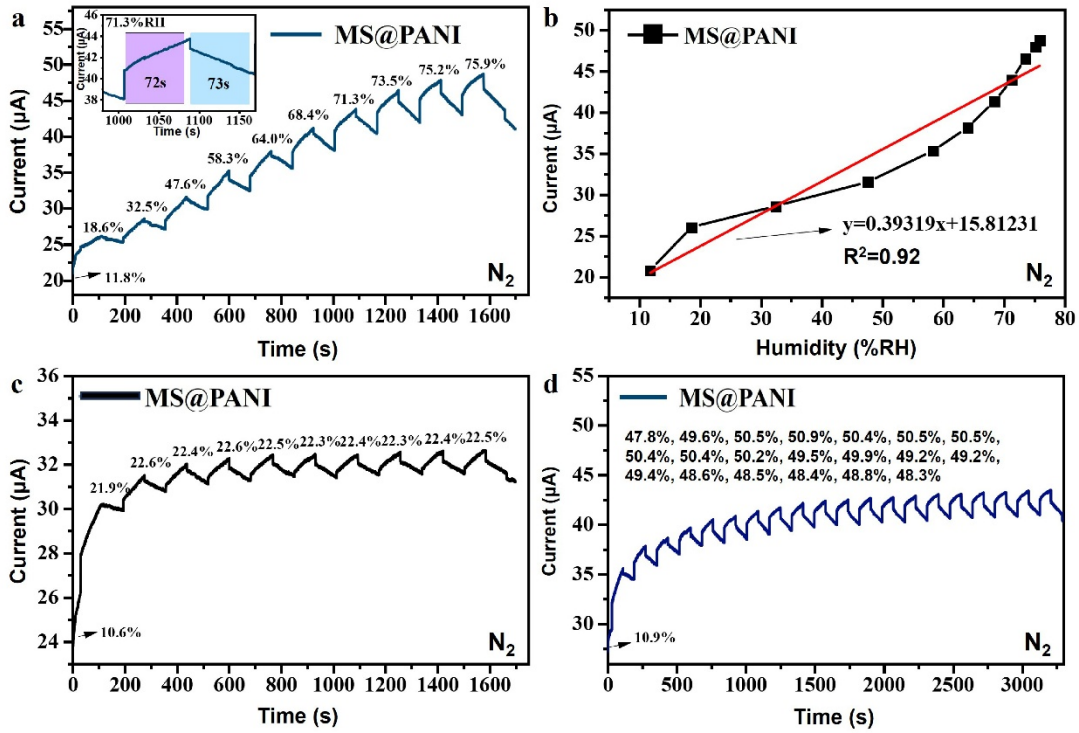

Fig. S9 In a N_2 background, the MS@PANI sensor is connected in series to an LED light and introduced into the testing circuit. a) Stepwise humidity current response curve. b) Fitting curve of current versus relative humidity. c) Ten cycles of testing. d) Twenty cycles of testing.

In N_2 environment, the MS@PANI sensor is connected in series with an LED light and integrated into the testing circuit. Fig. S6a depicts the stepwise humidity current response curve of the MS@PANI sensor with an LED light connected, with the inset detailing the response and recovery times of the MS@PANI sensor at 71.3 %RH humidity as 72 s and 73 s, respectively, under this circuit configuration. In Fig S6b, the linear fitting of the sensor's current values in relation to relative humidity is presented over an environmental range of 11.8% to 75.9%, exhibiting a linearity of 0.92. In Fig. S6c, ten cyclic tests are documented for the MS@PANI sensor connected in series with an LED light, conducted at approximately 22%RH. Subsequently, twenty cyclic tests were executed at around 50%RH, as illustrated in Fig. S6d. In summary, the test results under this circuitry configuration exhibit notable reproducibility and substantial linear sensitivity of the sensor to humidity changes.

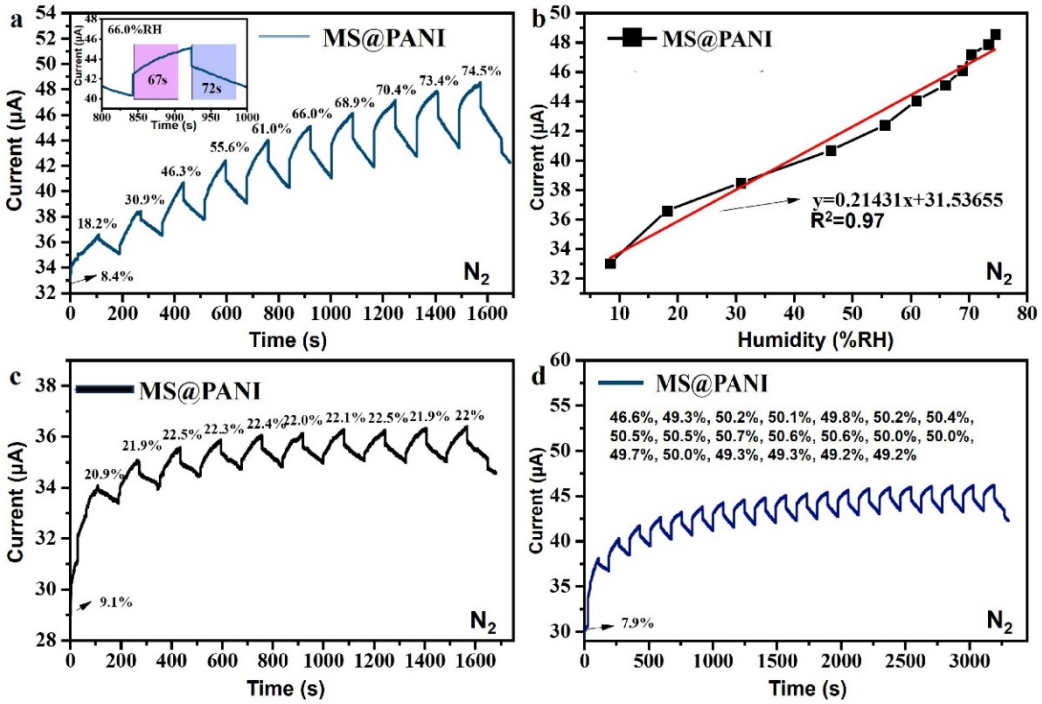

Fig. S10 In a N_2 background,, the MS@PANI sensor is connected in series with an LED light and powered by a commercial battery for the entire circuit, which is then integrated into the testing circuit. The panels show: a) stepwise humidity current response curve, b) fitting curve of current versus relative humidity, c) ten cyclic tests, and d) twenty cyclic tests.

In N_2 environment, the MS@PANI sensor was connected in series with an LED light and a commercial battery was used to power the entire circuit, which was then integrated into the testing circuit. The stepwise humidity current response curve of the MS@PANI sensor, powered by a commercial battery and connected to an LED light, is presented in Fig. S7a. The inset reveals that, under this circuit configuration, the response time and recovery time of the sensor at 66.0%RH humidity were 67 s and 72 s, respectively. In Fig. S7b, the linear fitting of the sensor's current values versus relative humidity is shown, spanning an environmental humidity range from 8.4%RH to 74.5%RH. The linear correlation coefficient R^2 is 0.97, indicating a high degree of linearity, and the sensitivity of the sensor is calculated to be 0.21 μA/%RH, suggesting a strong response to humidity changes. Fig. S7c documents ten cyclic tests performed on the MS@PANI sensor with the LED light, also powered by the commercial battery, at approximately 22%RH. Additionally, Fig. S7d illustrates twenty cyclic tests conducted under the same power supply conditions at approximately 50%RH. Overall, the cyclic tests carried out with this circuit configuration demonstrated excellent reproducibility.

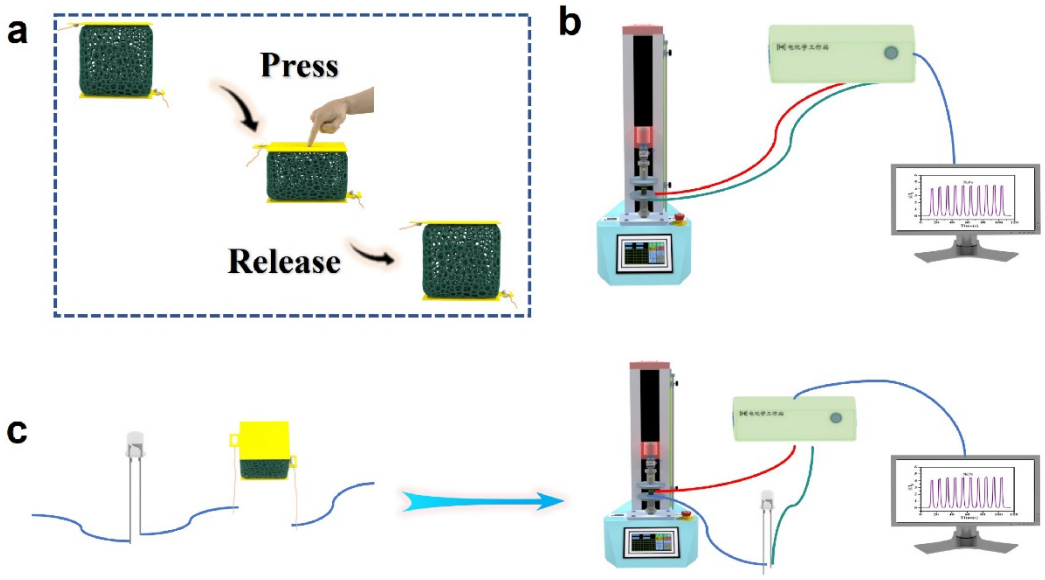

Fig. S11 a) Response mechanism of the MS@PANI sensor to pressure, (b-c) Performance tests for different circuit configurations.

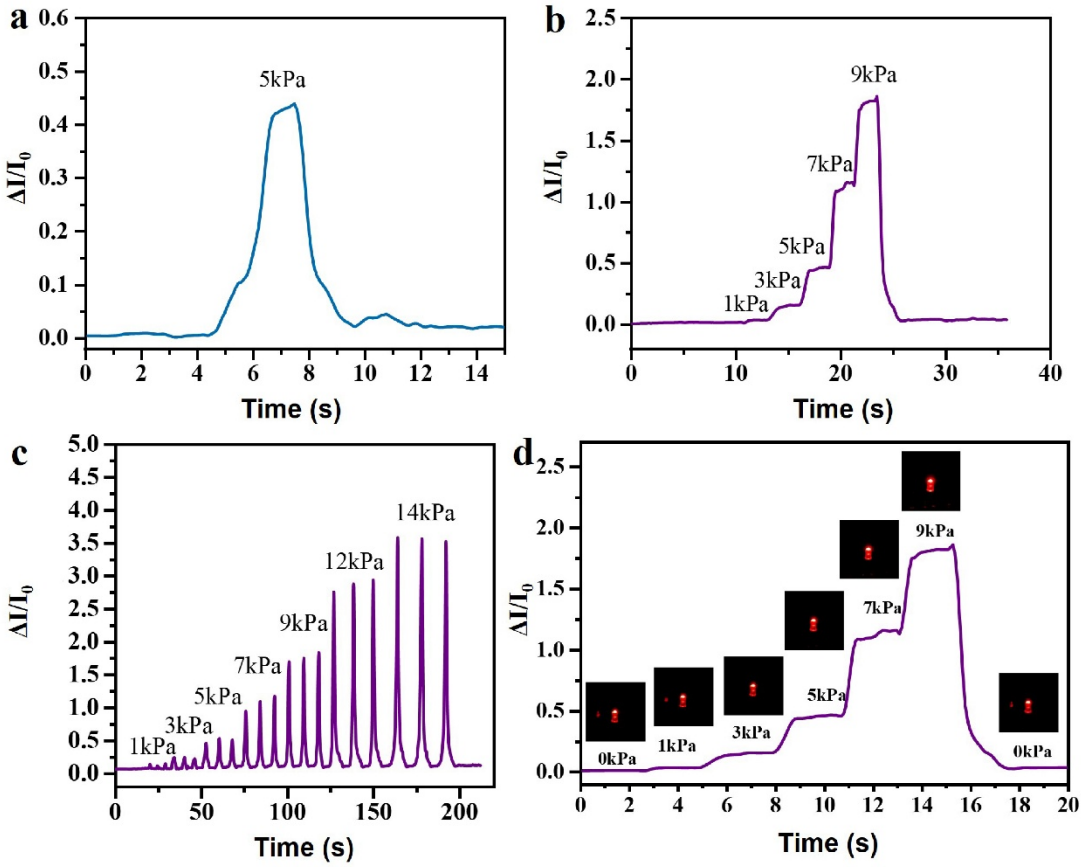

Fig. S12 MS@PANI was connected in series to the test circuit, a) response curve under 5 kPa pressure, b) ten cycles of loading-unloading response curve under 5 kPa pressure, c) response curve under step pressures of 1-14 kPa, d) step changes in pressure of 0-1-3-5-7-9-0 kPa, and the relative change in current and the process of LED brightness change were recorded.

Table S1. The comparison of MS@PANI humidity sensor with literatures.

Sensing material	Type	Detection range (%RH)	Response/ recovery (sec)	References
PANI/Chromium oxide	Resistive	20–90	134–213	1
PANI/Tin oxide	Resistive	5–95	26–30	2
PANI-holmium oxide	Resistive	11–97	32–46	3
Cupric oxide/polyaniline	Resistive	10–95	40–55	4
PANI-CMC	Impedance	25–75	10–90	5
PANI/NiO	Resistive	5–90	60–90	6
PANI/Paper	Resistive	0-97	220-150	7
MS@PANI	**Resistive**	**15-78**	**75-80**	**This work**

Table S2. The comparison of MS@PANI pressure sensor with literatures.

Working material	Sensitivity (kPa^{-1})	Pressure range (kPa)	reference
conductive biomass-based aerogels	1.41	0.032-2.5	8
graphene-polyimide foam	0.36	0-5	9
3 scale nested polypyrrole film	19.32	0.001-2	10
hierarchical graphene/ PDMS film	1.2	0-25	11
carbon NTs based sponge	0.01-0.02	0.01-1.2M	12
rGO/Polyaniline wrapped sponge	0.042-0.152	0-27	13
MS@PANI	**0.24**	**5-14**	**This work**

Reference:

1. K. C. Sajjan, M. Faisal, S. C. Vijaya Kumari, Y. T. Ravikiran and S. Khasim, AIP Conf. Proc., 2015, **1536**,289-292.
2. S. K. Shukla, S. K. Shukla, P. P. Govender and E. S. Agorku, *Micro. Acta*, 2015, **183**, 573-580.
3. S. Manjunatha, T. Machappa, Y. T. Ravikiran, B. Chethan and M. Revanasiddappa, Appl. Phys. A-Mater., 2019, **125**, 361-370.
4. P. Singh and S. K. Shukla, *Surfaces and Interfaces*, 2020, **18**，259-269.
5. S. Kotresh, Y. T. Ravikiran, H. G. Raj Prakash, C. V. V. Ramana, S. C. Vijayakumari and S. Thomas, *Cellulose*, 2016, **23**, 3177-3186.
6. P. Singh, C. S. Kushwaha, S. K. Shukla and G. C. Dubey, *Polym-Plast. Tech. Mat.* 2018, **58**, 139-147.
7. D. Y. Imali, E. C. J. Perera, M. N. Kaumal and D. P. Dissanayake, *RSC Advances*, 2023, **13**, 6396-6411.
8. J. Huang, D. Li, M. Zhao, H. Ke, A. Mensah, P. Lv, X. Tian and Q. Wei, *Chem. Eng. J.*, 2019, **373**, 1357-1366.
9. J. Yang, Y. Ye, X. Li, X. Lü and R. Chen, C.S.T.E., 2018, **164**, 187-194.
10. C. Yang, L. Li, J. Zhao, J. Wang, J. Xie, Y. Cao, M. Xue and C. Lu, *ACS Appl. Mater.*, 2018, **10**, 25811-25818.
11. J. Shi, L. Wang, Z. Dai, L. Zhao, M. Du, H. Li and Y. Fang, *Small*, 2018, **14**, 819-826.
12. S. Kim, M. Amjadi, T.-I. Lee, Y. Jeong, D. Kwon, M. S. Kim, K. Kim, T.-S. Kim, Y. S. Oh and I. Park, *ACS Appl. Mater.*, 2019, **11**, 23639-23648.
13. G. Ge, Y. Cai, Q. Dong, Y. Zhang, J. Shao, W. Huang and X. Dong, *Nanoscale*, 2018, **10**, 10033-10040.